

*School of Natural Sciences and Mathematics*

***Two ABC Transporters and a Periplasmic Metallochaperone Participate in Zinc Acquisition in Paracoccus Denitrificans***

UT Dallas Author(s):

Santosh Kumar

**Rights:**

Non-exclusive and nontransferable permission is granted to access and use this ACS article for non-commercial research and education purposes only, ©2018 American Chemical Society

**Citation:**

Neupane, Durga P., Santosh Kumar, and Erik T. Yukl. 2019. "Two ABC Transporters and a Periplasmic Metallochaperone Participate in Zinc Acquisition in Paracoccus denitrificans." *Biochemistry* 58(2): 126-136, doi: 10.1021/acs.biochem.8b00854

*This document is being made freely available by the Eugene McDermott Library of the University of Texas at Dallas with permission of the copyright owner. All rights are reserved under United States copyright law unless specified otherwise.*

## Two ABC Transporters and a Periplasmic Metallochaperone Participate in Zinc Acquisition in *Paracoccus denitrificans*

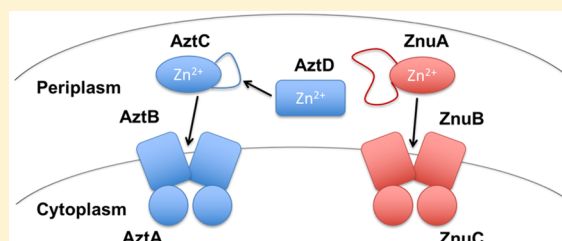
Durga P. Neupane,<sup>†</sup> Santosh Kumar,<sup>‡</sup> and Erik T. Yukl<sup>\*,†</sup>

<sup>†</sup>Department of Chemistry and Biochemistry, New Mexico State University, Las Cruces, New Mexico 88003, United States

<sup>‡</sup>Department of Biological Sciences, University of Texas at Dallas, Richardson, Texas 75080, United States

### Supporting Information

**ABSTRACT:** Bacteria must acquire the essential element zinc from extremely limited environments, and this function is performed largely by ATP binding cassette (ABC) transporters. These systems rely on a periplasmic or extracellular solute binding protein (SBP) to bind zinc specifically with a high affinity and deliver it to the membrane permease for import into the cytoplasm. However, zinc acquisition systems in bacteria may be more complex, involving multiple transporters and other periplasmic or extracellular zinc binding proteins. Here we describe the zinc acquisition functions of two zinc SBPs (ZnuA and AztC) and a novel periplasmic metallochaperone (AztD) in *Paracoccus denitrificans*. ZnuA was characterized *in vitro* and demonstrated to bind as many as 5 zinc ions with a high affinity. It does not interact with AztD, in contrast to what has been demonstrated for AztC, which is able to acquire a single zinc ion through associative transfer from AztD. Deletions of the corresponding genes singly and in combination show that either AztC or ZnuA is sufficient and essential for robust growth in zinc-limited media. Although AztD cannot support transport of zinc into the cytoplasm, it likely functions to store zinc in the periplasm for transfer through the AztABCD system.



Zinc is an essential trace element with catalytic, structural, and regulatory functions within proteins.<sup>1,2</sup> It is now well established that there exists a fierce competition for zinc at the interface between a mammalian host and bacterial pathogen.<sup>3</sup> The infected host employs several strategies to deplete both intracellular and extracellular levels of zinc available to the bacterium as a means of controlling the infection.<sup>4</sup> Thus, highly efficient zinc importers have been identified as critical for bacterial virulence. Several different types of import systems have been identified including siderophore-mediated zinc uptake in *Yersinia pestis*,<sup>5</sup> *Staphylococcus aureus*,<sup>6</sup> and *Pseudomonas aeruginosa*;<sup>7</sup> homologues of the eukaryotic ZIP transporters<sup>8</sup> called ZupT in *Salmonella enterica*<sup>9</sup> and *E. coli*;<sup>10</sup> import through a P-type ATPase in *P. aeruginosa*;<sup>11</sup> and a novel import system called ZevAB in *Haemophilus influenzae*.<sup>12</sup> However, the best studied and potentially most prevalent with regard to virulence come from the ATP binding cassette (ABC) family.<sup>13</sup>

ABC transporters are minimally composed of a membrane-bound permease and cytoplasmic ATPase.<sup>14,15</sup> Bacterial importers of this type also require a solute binding protein (SBP), which may be periplasmic, membrane tethered or fused to the permease.<sup>16</sup> The SBP specifically binds the appropriate substrate and transfers it to the permease for transport into the cytoplasm upon ATP hydrolysis by the ATPase.<sup>17</sup> SBPs exhibit a bilobed structure where substrate binding occurs between two structurally related  $\alpha/\beta$  domains. A structural classification of these proteins groups them into clusters (A–F) according to the nature of the linker between these two domains.<sup>18</sup> Some

clusters are further subdivided based on substrate specificity. The cluster A SBPs are characterized by a long  $\alpha$ -helix connecting the two domains and bind transition metals and transition metal complexes. Cluster A-I proteins directly bind zinc, manganese, or iron, while cluster A-II proteins bind transition metal complexes such as those formed with siderophores. In some cases, a single cluster A-I SBP and its associated transporter system (e.g., ZnuABC) are critical for virulence<sup>19–23</sup> making these particularly attractive targets for the development of novel antimicrobial drugs.

However, in other cases, zinc import is more complex. A number of organisms express more than one zinc ABC transporter, including the pathogens *Listeria monocytogenes*,<sup>24</sup> *Vibrio cholerae*,<sup>25</sup> and *Streptococcus* species.<sup>26–28</sup> In addition, periplasmic or extracellular metallochaperones appear to have a role in mediating zinc transport through ABC transporter systems. The N-terminal domain of the polyhistidine triad protein PhtD of *Streptococcus pneumoniae* has been shown to transfer zinc to the SBP AdcAII *in vitro*<sup>29</sup> and has been implicated in virulence.<sup>30,31</sup> Similarly, in some Gram-negative bacteria including *E. coli* and *Salmonella enterica*, the periplasmic zinc protein ZinT physically interacts with the SBP ZnuA<sup>32,33</sup> and is required for optimal growth in zinc-

**Special Issue:** Future of Biochemistry: The International Issue

**Received:** August 13, 2018

**Revised:** October 22, 2018

**Published:** October 24, 2018

limited media.<sup>33–35</sup> ZinT and ZnuA domains are found fused in a number of SBPs from *Streptococcal* species.<sup>36</sup> Both have been shown to bind zinc in *Streptococcus pneumoniae* and to be important for growth in zinc-limited media.<sup>27,37</sup> However, to our knowledge, no definite link between ZinT domains and virulence has yet been established. Nevertheless, a mechanistic understanding of the diversity and complexity of bacterial zinc acquisition systems will be essential to exploit these as antibacterial drug targets.

*Paracoccus denitrificans* is an excellent model system to study complex zinc acquisition for several reasons. First, it has two ABC transporter operons encoding cluster A-I SBPs, *znuABC* and *aztABCD*, which are transcriptionally regulated by the zinc uptake regulator (Zur) in response to zinc levels<sup>38</sup> (Figure 1,

**AztC: (117) GGGHYHYIDGKAVFHAG (133)**  
**ZnuA: (117) GGEHEHEHEHEHEHEHEHDGHHGHAEEQAAHHDHDSG (154)**

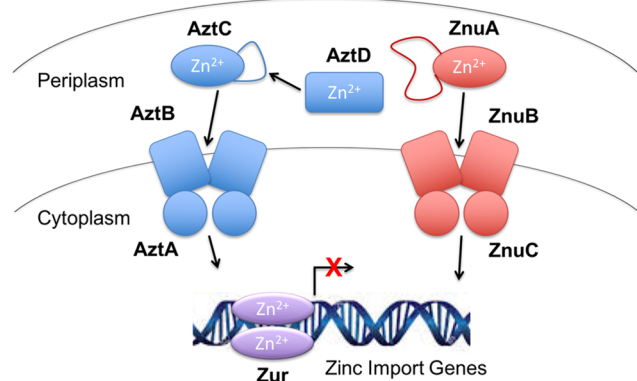


**Figure 1.** A simplified model for zinc acquisition and homeostasis through ABC transporters in *P. denitrificans*. Arrows show the direction of zinc transport. The flexible loops for the SBPs AztC and ZnuA are indicated in the figure, and their sequences are given. Underlined His residues in the AztC loop are required for zinc acquisition from the metallochaperone AztD.<sup>45</sup>

Figure S1). The SBPs AztC (UniProt KB A1B2F3) and ZnuA (UniProt KB A1B9L0) differ in the length and composition of a His-rich, flexible loop near the zinc binding site (Figure 1, Figure S2). Specifically, the AztC loop is approximately 17 residues in length with 3 His and 1 Asp residues, while the ZnuA loop is approximately 38 residues in length with 15 His and 14 Asp/Glu. This feature is common to zinc-specific cluster A-I SBPs,<sup>39,40</sup> and various functions have been postulated for it in different organisms.<sup>32,33,39,41–43</sup> Second, the *aztABCD* operon encodes a novel metallochaperone AztD (UniProt KB A1B2F4), which we have shown to stoichiometrically transfer zinc to the SBP AztC<sup>44</sup> (Figure 1). This process requires the presence of the AztC flexible loop and its three conserved His residues.<sup>45</sup> Finally, the periplasmic zinc binding proteins ZnuA, AztC, and AztD are highly conserved in pathogens belonging to the carbapenem-resistant Enterobacteriaceae (CRE), including *Klebsiella pneumoniae*. Thus, *P. denitrificans* presents an opportunity to understand the functions of distinct zinc SBPs as well as a periplasmic metallochaperone, which are likely to be relevant to these functions in human pathogens.

To date, the zinc binding and transfer properties of AztC and AztD have been well characterized *in vitro* (Table 1), but no work has been conducted on *P. denitrificans* ZnuA. Further, no studies on the *in vivo* functionality of any of these proteins have been undertaken in *P. denitrificans*. In this work, we have

**Table 1.** Zinc Binding Affinities for Periplasmic Zinc Binding Proteins from *P. denitrificans* as Determined by the Competition Assay with MF-2

protein	<i>n</i>	Zn $K_d$ (nM) $\pm$ SD ( <i>n</i> = 3)
WT ZnuA	2 <sup>a</sup>	1.0 <sup>a</sup>
	1 <sup>a</sup>	5.9 $\pm$ 1.1
	1 <sup>a</sup>	47 $\pm$ 33
	1 <sup>a</sup>	124 $\pm$ 154
$\Delta$ loop ZnuA	0.8 $\pm$ 0.1	0.3 $\pm$ 0.2
WT AztC <sup>46</sup>	0.9 $\pm$ 0.2	0.3 $\pm$ 0.1
$\Delta$ loop AztC <sup>45</sup>	1 <sup>a</sup>	0.2 $\pm$ 0.1
WT AztD <sup>44</sup>	2.2 $\pm$ 0.1	0.7 $\pm$ 0.3
		54 $\pm$ 8
		340 $\pm$ 110

<sup>a</sup>These values were fixed in the fitting protocol as described in the text.

characterized the metal binding properties of *P. denitrificans* ZnuA *in vitro* and evaluated the possibility of interaction with AztD. We have also explored the *in vivo* functions of AztC, AztD, and ZnuA in *P. denitrificans* by generating unmarked deletions of each gene alone and in combination. While AztD is not required for efficient zinc import and growth, it appears to be important for accumulation of zinc from limited environments, providing the first evidence of an *in vivo* function for this recently described periplasmic metallochaperone.

## EXPERIMENTAL PROCEDURES

**Expression and Purification of Proteins.** The intact gene encoding WT ZnuA was amplified by PCR from *P. denitrificans* PD1222 genomic DNA and cloned into pCDFDuet (Novagen) at the *NdeI* and *Acc65I/KpnI* restriction sites. The ZnuA loop deletion lacking residues 117–153 was generated using the Q5 Site-Directed Mutagenesis Kit (New England BioLabs) and confirmed by plasmid sequencing. Both WT and  $\Delta$ loop ZnuA plasmids were transformed into BL21 DE3 *E. coli* cells, which were grown in LB medium containing 50  $\mu$ g/mL streptomycin at 37 °C with shaking at 250 rpm to an OD<sub>600</sub> = 0.8–1.0. Overexpression was then induced by the addition of IPTG to 1.0 mM; the temperature was decreased to 20 °C, and the cells were grown with shaking overnight. Cells were harvested by centrifugation at 4000g for 25 min at 4 °C.

WT ZnuA was purified from the periplasmic fraction prepared using the osmotic shock protocol employed for AztC and AztD,<sup>46</sup> which was adapted from Wang et al.<sup>47</sup> Cells expressing  $\Delta$ loop ZnuA were lysed in 50 mM Tris pH 8.0, 150 mM NaCl, and 0.1 mM DTT. Both proteins were initially purified by anion exchange chromatography using the method previously described for WT AztC.<sup>46</sup> The peak containing WT ZnuA eluted at concentrations exceeding 350 mM NaCl, whereas  $\Delta$ loop ZnuA eluted between 300–350 mM NaCl. Fractions containing protein were combined, concentrated to <1 mL, and applied to a HiPrep Sephacryl S-200 HR size exclusion column (GE Healthcare) equilibrated with 50 mM Tris pH 8.0, 150 mM NaCl. After SEC, the proteins were highly pure as judged by SDS-PAGE. Both ZnuA and  $\Delta$ loop ZnuA concentrations were determined using an extinction coefficient at 280 nm of 38 687 M<sup>-1</sup> cm<sup>-1</sup> calculated as previously described.<sup>48</sup>

### Metal Quantitation and Generation of Apoproteins.

Protein samples at a concentration of 10–20  $\mu\text{M}$  were digested in 4 M  $\text{HNO}_3$  overnight at 70 °C and diluted 2.5-fold with Milli-Q water prior to metal analysis. For buffer samples, 2.5 mL were combined with 0.5 mL of concentrated  $\text{HNO}_3$  and digested overnight at 70 °C. Metal content was quantified using a PerkinElmer 2100 DV inductively coupled plasma optical emission spectrometer (ICP-OES), calibrated with a multielement standard (Alpha Aesar) at a wavelength of 213.857 nm for zinc, 238.204 nm for iron, and 257.610 nm for manganese. For zinc reconstitution, WT or  $\Delta\text{loop}$  ZnuA at 10  $\mu\text{M}$  and  $\text{ZnCl}_2$  at 200  $\mu\text{M}$  were combined at a final volume of 1 mL in 50 mM tris pH 8.0 and 150 mM NaCl and dialyzed against 1 L of this buffer at 4 °C overnight. Protein concentration was measured after dialysis, and zinc concentration in both the dialyzed protein sample and dialysis buffer was measured. The concentration of free zinc in the buffer was subtracted from that in the protein sample to determine the quantity of protein-bound zinc. Apoproteins were generated by dialysis at 4 °C against two changes of 500 mL of 50 mM NaOAc buffer pH 4.5, 50 mM EDTA, and 150 mM NaCl. This was followed by dialysis against two changes of 500 mL of 50 mM tris buffer pH 8.0, 150 mM NaCl, and 3.4 g/L Chelex. All samples were run in triplicate.

**Mag-Fura 2 Competition Assay.** Zinc binding affinities were measured using an MF-2 competition assay derived from Golynskiy et al.<sup>49</sup> as previously described.<sup>44,46</sup> All fluorescence measurements were made using a Varian Cary Eclipse fluorescence spectrophotometer with entrance and exit slits set to 10 nm. Protein concentration was measured before each experiment, and MF-2 concentration was determined using an extinction coefficient at 369 nm of 22 000  $\text{M}^{-1} \text{cm}^{-1}$ .<sup>49</sup> In each experiment, 1.0  $\mu\text{M}$  apoprotein and 0.5  $\mu\text{M}$  MF-2 were titrated with increasing concentrations of  $\text{ZnCl}_2$  or  $\text{MnCl}_2$ , keeping the total volume of titrant added less than 10% v/v. Fluorescence excitation spectra were scanned from 250–450 nm while monitoring emission at 505 nm. Experiments were performed in triplicate, and the fluorescence intensities at  $\lambda_{\text{ex}} = 330$  nm and  $\lambda_{\text{ex}} = 360$  nm were fit for zinc and manganese titrations, respectively, using the program DYNAFIT<sup>50,51</sup> and scripts adapted from Golynskiy et al.<sup>49</sup> Prior to each series of experiments, the affinity of MF-2 for zinc or manganese in our buffer system was determined using DYNAFIT and used in our calculation of protein binding affinity. The MF-2 affinity value for zinc varied from  $K_d = 92$ –141 nM between multiple experiments, while that for manganese was 1.8  $\mu\text{M}$ .

**Isothermal Titration Calorimetry (ITC).** ITC measurements were carried out on a Nano LV-ITC titration calorimeter (TA Instruments, Inc.). Apo-ZnuA was exchanged into degassed Chelex-treated 20 mM HEPES, pH 7.2, 200 mM NaCl, 5% glycerol using Zeba spin desalting columns and diluted to a final concentration of 30  $\mu\text{M}$  and volume of 200  $\mu\text{L}$  in this buffer. This was titrated with 1  $\mu\text{L}$  injections of 3.0 mM  $\text{ZnCl}_2$  in the same buffer for 30 injections at 25 °C and a stir speed of 250 rpm. A blank measurement to determine heats of dilution was conducted in the absence of protein. These were found to be negligible. Integrated heat data obtained for the protein titrations were directly analyzed using the multisite model in the NanoAnalyze software (TA Instruments).

**Zinc Transfer from AztD to Apo-ZnuA.** A HiTrap Q HP column (GE Healthcare) was prepared by washing with 50 mM EDTA pH 8.0 followed by equilibration with Chelex-

treated 20 mM tris pH 8.0. This same washing protocol was performed in between each sample run. In control experiments, 200  $\mu\text{L}$  of apo-ZnuA or holo-AztD at 150  $\mu\text{M}$  in Chelex-treated tris buffer was loaded onto the column and eluted on a gradient of NaCl. For Zn transfer experiments, apo-ZnuA and holo-AztD at 150  $\mu\text{M}$  each were incubated for 15 min at room temperature prior to loading onto the column. For control experiments, the ZnuA (38 687  $\text{M}^{-1} \text{cm}^{-1}$ ) and AztD (33 666  $\text{M}^{-1} \text{cm}^{-1}$ ) extinction coefficients were used to convert absorbance values to concentrations on the UV chromatogram. Given the similarity of these values, an averaged value was used for the transfer experiment. SDS-PAGE was used to confirm the identity of protein found in each chromatographic fraction. Fractions were collected and digested in 4 M  $\text{HNO}_3$  for Zn content analysis by ICP-OES.

**Bacterial Strains and Culture Conditions.** The *in vivo* functional characterizations of AztC, AztD, and ZnuA were performed using *P. denitrificans* PD1222 or its mutant derivatives. *Escherichia coli* DH5 $\alpha$  (New England Biolabs) cells were used for basic cloning. BL21 (DE3) cells were used for heterologous expression of *P. denitrificans* proteins, while *E. coli* S17–1 and *E. coli* having pRK2013 were used to generate knockout strains of *P. denitrificans* by triparental mating. *P. denitrificans* was grown at 30 °C in defined media as previously described<sup>38</sup> unless otherwise mentioned, while *E. coli* was grown at 37 °C in LB with appropriate antibiotics.

**Generation of *P. denitrificans* Mutants.** Unmarked deletions of *aztC*, *aztD*, *aztCD*, and *znuA* were generated by double crossover homologous recombination using the suicide plasmid pK18mobSacB<sup>52</sup> by the method described previously.<sup>53</sup> Briefly, the procedure involves the PCR amplification of 600–800 bp fragments flanking the target genes. These are cloned into pK18mobSacB after cleavage at a single site by *EcoRI* restriction endonuclease and then ligated together by overlapping regions added in the primers.<sup>54</sup> Each pK18mobSacB derivative with suitable DNA fragments was confirmed by sequencing and transformed into *E. coli* S17–1 cells. Triparental mating was employed to mobilize pK18mobSacB from *E. coli* S17–1 into *P. denitrificans* in the presence of helper plasmid pRK2013 after growing all cells to the stationary phase. *P. denitrificans* 1222 is rifampicin-resistant, while both pK18mobSacB and pRK2013 confer kanamycin resistance. Single crossover recombinants were selected on the basis of both rifampicin and kanamycin resistance. These transconjugants were grown in salt-free LB with no antibiotics to the stationary phase, and double crossover events were selected on LB-agar plates supplemented with 6% sucrose (w/v); sucrose-resistant isolates were screened for a loss of kanamycin resistance. The presence of the appropriate deletion was confirmed by PCR and by sequencing of the PCR product.

**Determination of Growth and Metal Content in *P. denitrificans*.** WT and mutant cells were grown overnight in defined media containing 10  $\mu\text{M}$   $\text{ZnCl}_2$ . One mL of overnight cultures was washed once and resuspended in media with no added zinc. These were used to inoculate duplicate media conditions containing no added zinc, 50  $\mu\text{M}$   $\text{ZnCl}_2$ , or 50  $\mu\text{M}$  of the zinc chelator *N,N,N',N'*-tetrakis(2-pyridylmethyl)-ethylenediamine (TPEN) to an OD<sub>600</sub> of 0.02. Growth of cells was monitored by measuring the optical density at 600 nm over time in hours. Cellular metal accumulation was expressed in nanogram of metal per milligram of dry cell weight. For this, 3–10 mL of WT and mutant *P. denitrificans* cells grown overnight in different media conditions were

pelleted at 4000g for 5 min, washed three times with phosphate buffered saline (PBS), centrifuged as above, and dried at 105 °C in preweighed microcentrifuge tubes to a constant weight (4–20 mg). Net cell weight was recorded, and the cells were digested in 250  $\mu$ L of concentrated HNO<sub>3</sub> for 3 h at 70 °C followed by dilution to 2.5–4.0 mL with nanopure water. Metal content was quantified by ICP-OES as described above. All samples were run in triplicate.

Statistical analyses were done in R statistical software (R Core Team 2018).<sup>55</sup> One-way Analysis of Variance (ANOVA) was used to compare the variance in the mean zinc content between strains grown in the same condition. Following the significance of ANOVA test, we used TukeyHSD test to compare the mean difference in metal content between WT and mutant strains.

**Reverse Transcription PCR (RT-PCR).** WT and mutant cells were grown in media with no added zinc to an OD<sub>600</sub> of 0.4–0.5. Two mL of 5% v/v phenol in ethanol was added to 5 mL cells, chilled on ice for 30 min, and centrifuged, and the pellet was stored at –80 °C. RNA was extracted using a PureLink RNA Mini Kit (Ambion). DNA contamination was removed using an on-column DNase digestion protocol (Invitrogen). RNA concentration and purity were determined spectrophotometrically using a Nano drop Spectrophotometer ND-1000. cDNA was synthesized from 800 ng of pure RNA in 20  $\mu$ L reaction volume using the SuperScript III first-strand synthesis kit (Invitrogen). One  $\mu$ L of cDNA at a concentration of 40 ng/ $\mu$ L was used as a template for PCR reactions using primers designed to amplify the entire *aztD* gene.

## RESULTS

**In Vitro Analysis of Zinc Binding to ZnuA.** Untagged full-length ZnuA and a loop deletion mutant ( $\Delta$ loop ZnuA) lacking residues 117–153 (Figure 1) were heterologously expressed in *E. coli* and purified to homogeneity by anion exchange and size exclusion chromatography (SEC). SEC indicated that both proteins migrate exclusively as monomers, and both were judged as highly pure using SDS-PAGE (Figure 2). WT ZnuA contained 0.08–0.20 zinc equivalents as isolated. However, reconstitution of WT ZnuA with excess zinc chloride followed by dialysis resulted in protein containing 5.7 equiv of zinc. This same procedure using  $\Delta$ loop ZnuA resulted in 1.3 equiv of zinc. This gave the first indication that *P. denitrificans* ZnuA is capable of binding multiple zinc ions and that these extra zinc binding sites are likely found on the flexible loop.

To prepare the proteins for metal binding assays, any bound metal was removed as described above to generate apoproteins containing <0.05 equiv of zinc as determined by ICP-OES. Competition assays with the fluorescent metal binding probe Magfura-2 (MF-2) were employed<sup>49</sup> (Figure 3) to specifically assign stoichiometry and affinity of zinc binding sites for both proteins. Using the affinity of MF-2 as determined in our buffer system, a good fit for the WT data required five zinc binding sites (Table 1). It should be noted that, while this analysis provides individual binding affinities for each site, it is unable to reliably distinguish binding sites of similar affinity. Similarly, it cannot accurately determine  $K_d$ 's for those sites with affinities significantly different from that of the competitor. Thus, in this case where there are five detectable binding events, there are multiple equivalent fitting solutions. With this in mind, two binding sites exhibit very high, indistinguishable affinities to which we have assigned values of 1 nM. The

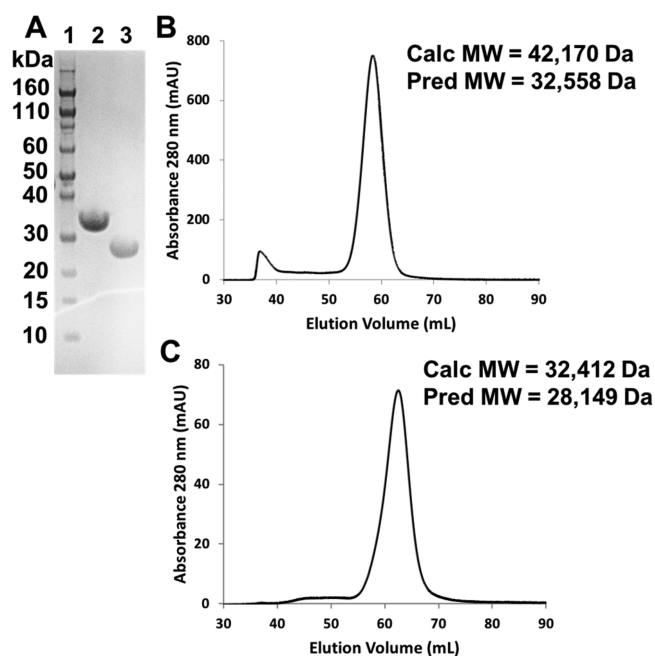


**Figure 2.** Purification of WT and  $\Delta$ loop ZnuA. (A) SDS-PAGE gel: lane 1, MW standard; lane 2, purified WT ZnuA; lane 3, purified  $\Delta$ loop ZnuA. Size exclusion chromatograms of (B) WT and (C)  $\Delta$ loop ZnuA. Predicted MW refers to that determined from the primary sequence, while calculated MW is determined from elution time in comparison with a set of known standards.

remaining three sites exhibited sufficiently different  $K_d$  values within the range of the MF-2 assays to allow them to be determined by fitting. This analysis indicates that WT ZnuA binds two zinc ions with a very high affinity ( $K_d \leq 1$  nM) and three others with affinities in the low to midnanomolar range. On the other hand, the  $\Delta$ loop ZnuA data fit best to a single binding site model, again consistent with equilibrium dialysis results. Although the affinity for the primary zinc binding site is essentially unaltered by deletion of the loop, the number of zinc binding sites is drastically reduced, localizing these additional sites to the flexible loop.

Some cluster A-I solute binding proteins exhibit similar binding affinities for both zinc and manganese<sup>56–59</sup> and may have dual functions in metal homeostasis.<sup>57</sup> Therefore, we also evaluated the *in vitro* manganese binding affinity for ZnuA using the MF-2 competition assay. However, manganese binding could not be detected by this assay, indicating that if manganese does bind to ZnuA it does so with a significantly lower affinity than does MF-2 ( $K_d \gg 1$   $\mu$ M). Combined with the observation that expression of *znuA* depends on zinc and not manganese levels,<sup>38,46</sup> these results strongly indicate that ZnuA functions solely in zinc homeostasis.

Isothermal titration calorimetry (ITC) was used to further characterize zinc binding to ZnuA (Figure 4). ITC titration of apo-WT ZnuA (Figure 4A,B) with zinc yields a very complex isotherm indicative of multiple binding events. Initial binding events up to 2 equiv of added zinc are high affinity and exothermic. Between 2 and 5 equiv of zinc, an endothermic transition becomes predominant and decays gradually, indicative of additional binding sites with a lower affinity. Three classes of binding sites were required to adequately fit this data (Figure 4B, Table 2). Sites 1 and 2 each bind multiple zinc ions with a low nanomolar affinity and opposite signs of  $\Delta H$ . Site 1 binding is exothermic while site 2 is endothermic.

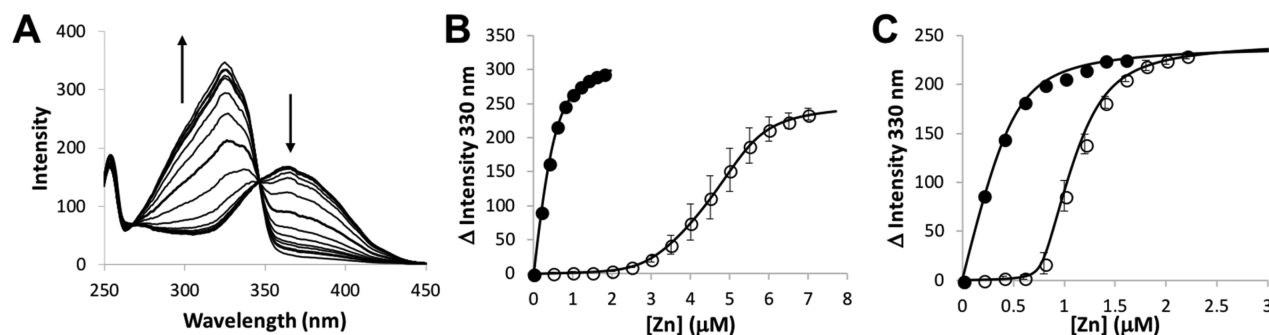


**Figure 3.** Zinc binding by WT and  $\Delta$ loop ZnuA by MF-2 competition assay. (A) Example of a MF-2 assay containing  $0.5 \mu\text{M}$  MF-2 and  $1.0 \mu\text{M}$  apo-WT ZnuA. Arrows indicate the direction of fluorescence changes upon titration with increasing zinc. Intensity change at 330 nm with increasing zinc in the absence (solid circles) and presence (empty circles) of (B) apo-WT ZnuA and (C)  $\Delta$ loop ZnuA. Titrations containing WT or  $\Delta$ loop ZnuA were performed in triplicate, and error bars represent the standard error between experiments. Fits are shown as solid lines.

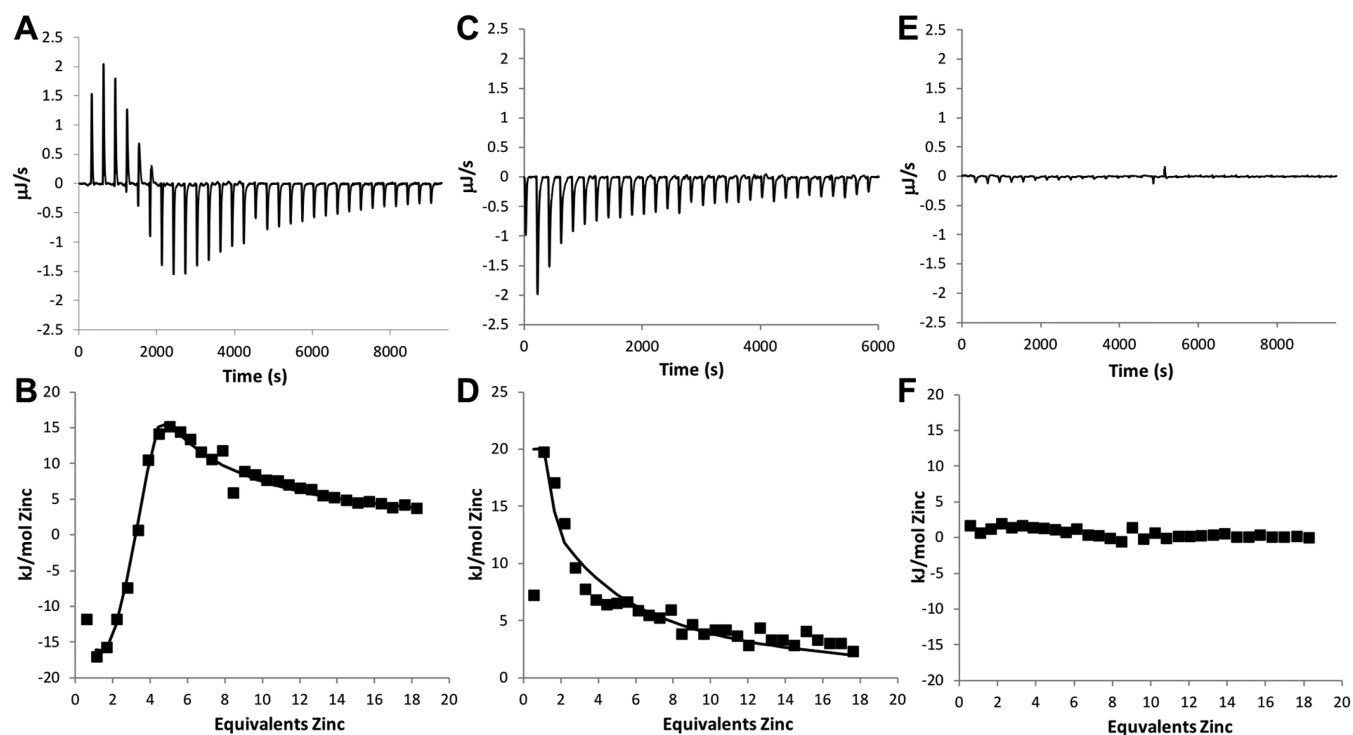


**Figure 4.** Zinc binding by WT and  $\Delta$ loop ZnuA by ITC. ITC isotherms and integrated heats of titration of  $30 \mu\text{M}$  WT ZnuA (A and B),  $\Delta$ loop ZnuA (C and D), or a buffer blank (E and F) titrated with  $3.0 \text{ mM}$   $\text{ZnCl}_2$ . Solid lines represent fits to the data resulting in binding parameters listed in Table 2.

**Table 2.** *P. denitrificans* ZnuA Zinc Binding Parameters as Determined by ITC<sup>a</sup>

protein	site	<i>n</i>	$\Delta H$	$K_a$ ( $\text{M}^{-1}$ )	$K_d$ (nM)
WT ZnuA	1	$2.4 \pm 0.3$	−	$5.3 \times 10^8 \pm 2.5 \times 10^8$	1.9
	2	$1.9 \pm 0.4$	+	$1.2 \times 10^8 \pm 2.5 \times 10^8$	8.3
	3	$0.1 \pm 1.4$	+	$6.4 \times 10^3 \pm 5.0 \times 10^3$	$156 \mu\text{M}$
$\Delta$ loop ZnuA	1	$1.2 \pm 0.3$	+	$1.0 \times 10^8 \pm 6.3 \times 10^8$	10
	2	$0.3 \pm 3.4$	+	$3.6 \times 10^3 \pm 9.1 \times 10^3$	$278 \mu\text{M}$

<sup>a</sup>Uncertainties are derived from the fit at the 95% confidence interval.

Site 3 binds zinc with low affinity, positive  $\Delta H$  and a large uncertainty on *n*. The values extracted from this analysis should be treated with caution, due to the large number of fitted parameters. In particular, *n* and  $\Delta H$  are linked parameters, and  $\Delta H$  refined to physically unreasonable values, which are consequently not reported. Similar difficulties with

fitting this type of ITC data have been noted elsewhere.<sup>42,60</sup> Nevertheless, the ITC data are consistent with MF-2 competition assays, indicating that ZnuA binds multiple zinc ions with affinities in the nanomolar range.

ITC data for apo- $\Delta$ loop ZnuA (Figure 4C,D) consists of solely endothermic transitions and appears biphasic. Although the fit for two binding sites is not of excellent quality, it indicates the presence of a single, endothermic high-affinity binding site and adventitious binding similar to what was observed for the WT. This is consistent with MF-2 data, which unequivocally demonstrates that deletion of the loop removes all but one high-affinity binding site. A blank titration indicated that heats of dilution for  $\text{ZnCl}_2$  in buffer were insignificant (Figure 4E,F), confirming that the low-affinity zinc binding is a property of both WT and  $\Delta$ loop ZnuA, although unlikely to be physiologically relevant.

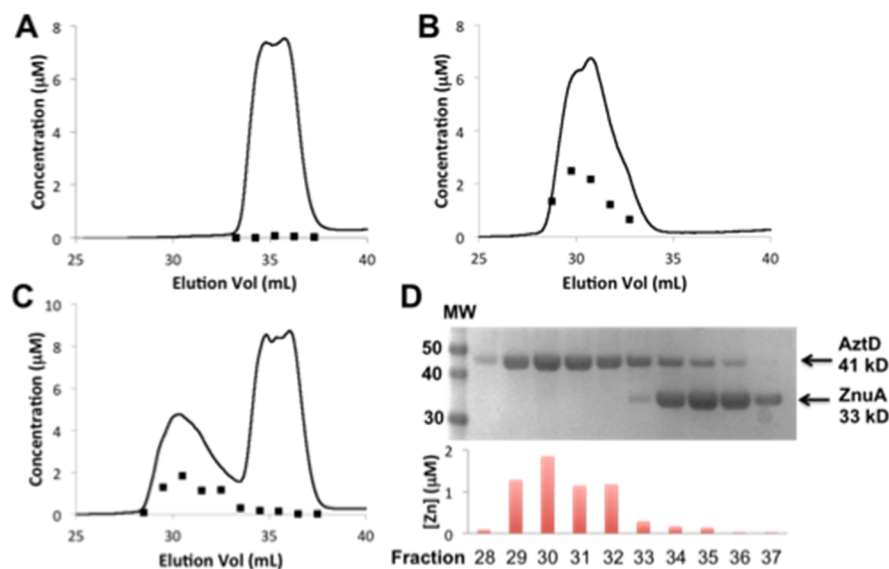


**Figure 5.** Zinc transfer from AztD to WT apo-ZnuA. (A) Apo-WT ZnuA, (B) holo-AztD, and (C) an equimolar mixture were applied to an ion exchange column, and the protein eluted with increasing [NaCl]. The protein was detected by absorbance at 280 nm and converted to concentration using extinction coefficients (solid line) as described in above. One mL fractions were collected and analyzed for zinc content (filled squares). (D) Fractions from C were run on SDS-PAGE and bands compared with zinc content.

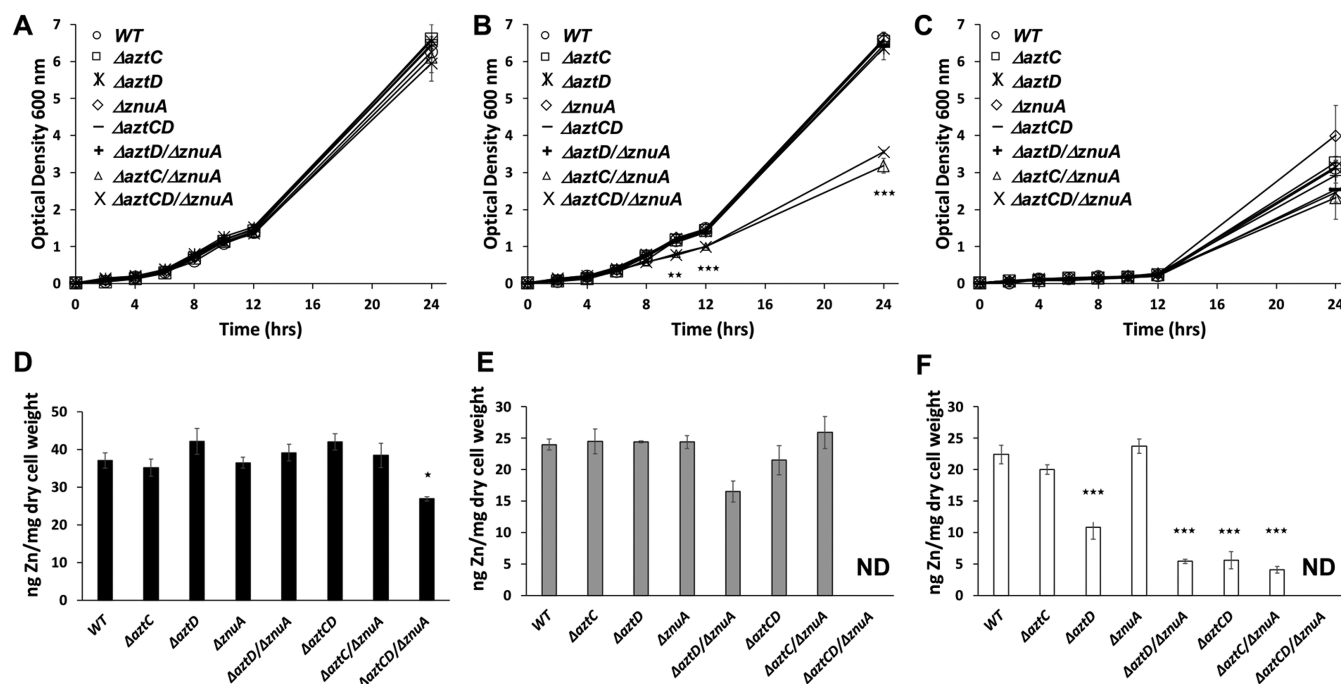


**Figure 6.** (A, B, and C) Growth curves and (D, E, and F) quantitation of cellular zinc for WT and mutant *P. denitrificans* strains grown in zinc-repleted (A and D, black bars), zinc-limited (B and E, gray bars), and zinc-chelated (C and F, white bars) media. Growth data are presented as the average values for duplicate experiments with error bars representative of the standard deviation. Zinc quantitation is presented as the average values for triplicate experiments with error bars representative of the standard error between replicates. TukeyHSD test was used to evaluate statistical significance of differences. For growth curves, OD<sub>600</sub> of each mutant strain was compared to WT. Zinc content was compared between strains grown in a given condition. Significance is indicated as follows: \**p* < 0.05, \*\**p* < 0.01, \*\*\**p* < 0.001. ND = not detected, indicating that zinc content was below the detection limit, which for these samples is approximately 2 ng/mg dry cell weight.

Finally, we sought to determine if zinc transfer occurs from the zinc chaperone AztD to ZnuA. Transfer of zinc from AztD to AztC was previously determined by incubation of AztD as-isolated containing 0.5–0.7 equiv of zinc with apo-AztC followed by separation by SEC and analysis of zinc content in chromatographic fractions by ICP-OES.<sup>44</sup> AztD was not reconstituted prior to the experiment to avoid the possibility

of nonspecific transfer from adventitious binding. In this case, transfer appeared to be virtually stoichiometric and directional. The same approach was followed to assay transfer to apo-ZnuA except that ion exchange chromatography was used to separate the two proteins since AztD and ZnuA coelute in SEC. To exclude the chance of cross-contamination with zinc during anion exchange chromatography, apo-ZnuA (Figure 5A) and

holo-AztD (Figure 5B) were first run separately. This control demonstrates that apo-ZnuA does not acquire zinc nor does zinc dissociate from holo-AztD during chromatography.<sup>44</sup> When combined, the proteins elute separately, indicating that no stable complex is formed between them (Figure 5C). Further, zinc remains associated exclusively with the AztD-containing fractions (Figure 5C,D). Thus, we conclude that AztD cannot transfer zinc to ZnuA, indicating that productive interaction with AztC<sup>44</sup> is mediated by specific protein–protein contacts.

**Growth and Metal Accumulation of WT and Mutant *P. denitrificans*.** Unmarked in-frame deletions of *P. denitrificans* *aztC*, *aztD*, and *znuA* were generated individually and in combination as described above. Phenotypes were evaluated by growth in media containing no added zinc (zinc-limited), 50  $\mu$ M ZnCl<sub>2</sub> (zinc-repleted), or 50  $\mu$ M of the zinc chelator TPEN (zinc-chelated). Despite treatment with Chelex, zinc content in zinc-limited media averaged  $\sim$ 0.5  $\mu$ M, likely due to zinc impurities in other metal salts and leaching from laboratory equipment.<sup>35,61</sup> Nevertheless, a previous study showed these zinc-limited conditions to be sufficient to significantly upregulate zinc acquisition genes under the control of the zinc-dependent transcriptional regulator Zur.<sup>38</sup> Further, all culture conditions contained 126  $\mu$ M EDTA, which should further limit zinc availability in zinc-depleted conditions. To rule out polar effects on *aztD* expression as a result of *aztC* deletion, RT-PCR was performed on WT,  $\Delta$ *aztC*/ $\Delta$ *znuA*, and  $\Delta$ *aztCD*/ $\Delta$ *znuA* strains grown in zinc-limited media (Figure S3). The intact *aztD* gene was amplified from WT and  $\Delta$ *aztC*/ $\Delta$ *znuA* strains, while no expression was observed for the  $\Delta$ *aztCD*/ $\Delta$ *znuA* negative control. Moreover, expression appears higher in the  $\Delta$ *aztC*/ $\Delta$ *znuA* strain than the WT, suggesting a lower intracellular zinc concentration in this mutant.

All strains exhibited comparable growth in zinc-repleted conditions, and only  $\Delta$ *aztCD*/ $\Delta$ *znuA* accumulated significantly less zinc than WT (Figure 6A,D). In zinc-limited conditions (Figure 6B,E), only  $\Delta$ *aztC*/ $\Delta$ *znuA* and  $\Delta$ *aztCD*/ $\Delta$ *znuA* exhibited a significant growth defect. Intriguingly, while zinc accumulation by the  $\Delta$ *znuA*/*aztC* double mutant was not significantly different from WT, the  $\Delta$ *znuA*/ $\Delta$ *aztCD* triple mutant was significantly lower in replete conditions and below the detection limit (approximately 2 ng/mg dry cell weight) in zinc-limited conditions.

The growth of all strains was equally attenuated in zinc-chelated media. Although there is some variability in OD<sub>600</sub> values after 24 h between strains, none of these exhibited a statistically significant difference from WT. However, the  $\Delta$ *aztC*/ $\Delta$ *znuA* strain as well as any strain harboring a deletion of *aztD* accumulated significantly less zinc under these conditions than WT (Figure 6C,F). Here again, zinc levels in the triple mutant were below the detection limit. To confirm this finding and determine whether zinc limitation dysregulates acquisition of other essential metals, manganese and iron were also measured in WT,  $\Delta$ *aztC*/ $\Delta$ *znuA*, and  $\Delta$ *aztCD*/ $\Delta$ *znuA* strains (Figure 7). Iron levels were constant for these strains across all conditions. However, manganese levels increased dramatically in all three strains in the presence of TPEN.

In total, the growth and zinc accumulation data suggests that either AztC or ZnuA is necessary and sufficient for zinc import to support WT growth under zinc-limited conditions. AztD does not appear to have an essential role in importing zinc into the cytoplasm. However, it does function to accumulate zinc

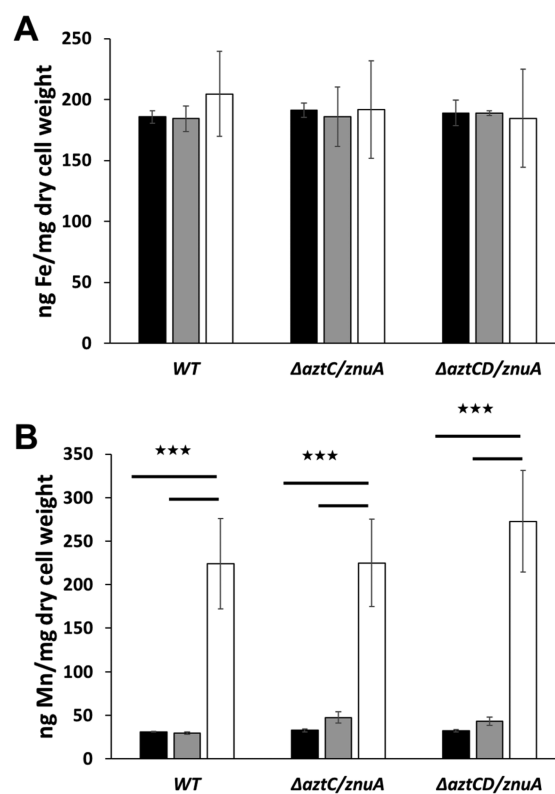


**Figure 7.** Quantitation of cellular (A) iron and (B) manganese for WT and mutant *P. denitrificans* strains in zinc-repleted (black bars), zinc-limited (gray bars) and zinc-chelated (white bars) media. Data are presented as the average values for triplicate experiments with error bars representative of the standard error between replicates. TukeyHSD test was used to evaluate statistical significance of differences in metal content as follows: \* $p < 0.05$ , \*\* $p < 0.01$ , \*\*\* $p < 0.001$ .

even in the absence of high-affinity transport and in the presence of TPEN.

## DISCUSSION

The cluster A-I SBPs bind a single metal ion at a cleft between two structurally related  $\alpha/\beta$  domains, typically with a low nanomolar affinity. Many zinc-specific ZnuA homologues also contain a flexible loop rich in His and Asp/Glu residues, which can provide additional zinc binding sites (Figure S2). In ZnuA from *E. coli*,<sup>62</sup> *S. enterica*,<sup>32</sup> and *P. aeruginosa*<sup>63</sup> binding of a single zinc to the loop with a relatively low affinity ( $\mu$ M range) was detected in addition to binding to the high-affinity site (nM range). ZnuA from *Treponema pallidum*<sup>56</sup> has a loop of comparable size yet binds multiple zinc ions, although the exact stoichiometry is not precisely defined. In ZnuA homologues with very long, His-rich loops such as those from *Hemophilus influenzae*<sup>19</sup> and *Synechocystis* 6803,<sup>42</sup> multiple zinc binding events have also been observed. Although binding affinities were not determined for the *H. influenzae* ZnuA, the other two proteins were characterized by ITC. Each exhibited a high-affinity (nM range) binding of two zinc ions as well as additional (up to 6 in the case of *Synechocystis*) low-affinity ( $\mu$ M range) binding events. In both cases, each transition was exothermic, and mutagenesis studies on *Synechocystis* ZnuA further localized all low-affinity binding sites to the flexible loop.

In contrast, MF-2 assay and equilibrium dialysis indicate that *P. denitrificans* ZnuA binds up to 5 zinc ions with nM affinity with 4 of these sites localized to the flexible loop. As noted above, ITC data for multiple binding events is difficult to analyze quantitatively. However, ITC results are consistent with multiple high-affinity binding sites and further demonstrate that zinc binding results in both endothermic and exothermic transitions. In particular, data with  $\Delta$ loop ZnuA indicates that binding of a single zinc ion to residues of the conserved binding pocket is entropically driven.

The reason for the enhanced zinc binding affinity of the *P. denitrificans* ZnuA flexible loop relative to that of *Synechocystis* may reside in the sequence of the loop rather than its length, which is similar in both proteins (Figure S2). In particular, the *P. denitrificans* ZnuA loop is significantly richer in His residues with 15 versus 8 in *Synechocystis*. To our knowledge, all of the zinc-specific cluster A-I SBPs coordinate zinc at the high-affinity site through a 3 His, 1 Asp/Glu/H<sub>2</sub>O ligand set<sup>64</sup> and His is highly represented in biological zinc sites.<sup>65</sup> An increased number of His ligands may result in higher affinity binding sites by allowing more zinc ions to adopt a preferred coordination. In that regard, it is interesting to note that the *H. influenzae* ZnuA loop contains 23 His residues (Figure S3). Although affinities for this protein were not specifically determined, extensive dialysis after zinc reconstitution demonstrated binding of up to 5 zinc ions, while dialysate zinc concentrations were <1  $\mu$ M,<sup>19</sup> suggesting a nM range affinity.

Although the above results provide an interesting contrast in the thermodynamics with which different ZnuA homologues bind multiple zinc ions, they do little to elucidate the function of the flexible loop. As with other cluster A-I SBPs,<sup>42,45</sup> its deletion in *P. denitrificans* ZnuA does not impair binding at the high-affinity site, contradicting a role as a zinc chaperone. The relatively short loop of *P. denitrificans* AztC is also flexible as indicated by absent<sup>46</sup> or weak<sup>45</sup> electron density in crystal structures. It does not bind additional zinc but has been shown to mediate interaction with and subsequent metal transfer from the metallochaperone AztD.<sup>45</sup> However, we have shown here that ZnuA does not interact with AztD, ruling this out as a possible function. Given the unusually high affinity of the extra zinc binding sites of *P. denitrificans* ZnuA, it is tempting to speculate that this feature functions in zinc storage. Whether binding between sites is dynamic, with transfer occurring between them, is unknown. Unfortunately, this is very difficult to test. Nevertheless, it has been suggested that a long, His-rich loop may function to sequester zinc ions from the periplasm, passing them to the high-affinity site for transfer to the permease as zinc concentrations fall.<sup>19,41,56</sup> A regulatory function for the loop acting as a sensor of high zinc concentrations has also been proposed.<sup>42</sup> We are currently working to evaluate these possible functions by complementation of *P. denitrificans* knockout strains with loop deletion ZnuA variants.

Growth assays and intracellular zinc accumulation of single *aztC*, *znuA*, and *aztD* knockout strains show that none of these proteins are required for growth under replete zinc conditions. The expression of zinc ABC transporters is strongly repressed under such conditions by the zinc-dependent transcription factor Zur,<sup>23,38,66</sup> and other low-affinity transport mechanisms are likely active. *P. denitrificans* encodes an NRAMP family transporter<sup>38</sup> that may function in this capacity. Conversely, either ZnuA or AztC is essential for WT growth under zinc-

limiting conditions, consistent with the role of ABC transporters in high-affinity zinc import. These results further suggest that the AztABCD and ZnuABC transporters have redundant functions, at least for *P. denitrificans* in zinc-limited liquid media. However, it should be noted that the appearance of functional redundancy likely depends on the environment in which it is tested. For example, *Streptococcus pneumoniae* encodes two cluster A-I SBPs, which appear to have redundant functions supporting growth and zinc acquisition from liquid media,<sup>67</sup> yet both are required for full virulence in a mouse infection model.<sup>27</sup> Similar observations have been made for the two zinc transporters in *Listeria monocytogenes*.<sup>24</sup> As *P. denitrificans* is a highly versatile organism capable of growth in a variety of soil and aqueous environments,<sup>68</sup> it seems likely that AztABCD and ZnuABC may not be functionally redundant in all of them. In particular, soils can vary dramatically in total zinc content<sup>69</sup> and speciation.<sup>70</sup> Multiple zinc transporters may allow access to a greater variety of soil environments. Similarly, it will be of interest to evaluate whether the homologous transporters in CRE pathogens are redundant in liquid media versus animal infection models.

AztD was not able to substitute for either SBP to restore growth. However, deletion of AztD in the  $\Delta$ aztC/ $\Delta$ znuA background led to a dramatic decrease in the amount of cellular zinc under zinc-limited conditions. Further, any mutant harboring a deletion of *aztD* accumulated significantly less zinc in zinc-chelated conditions. Our hypothesis is that AztD is capable of sequestering and accumulating zinc in the periplasmic space but is unable to independently mediate its transport into the cytoplasm to support growth. This explains why the  $\Delta$ aztC/ $\Delta$ znuA mutant still accumulated WT levels of zinc (presumably binding to AztD in the periplasm), even though its growth was attenuated. Transcription of *aztD* is the most highly upregulated of any gene in the *P. denitrificans* genome under conditions of zinc limitation,<sup>38</sup> indicating that this organism responds to these conditions in part by increasing its capacity for periplasmic zinc storage. As mentioned above, the high zinc binding capacity of ZnuA suggests that it may have some function in this context as well.

Interestingly, the presence of TPEN did not inhibit growth of any mutants relative to the WT. We have repeatedly observed that *P. denitrificans* cells can recover from TPEN growth inhibition over time and that recovery does not require either zinc ABC transporter. They may be able to utilize this membrane permeable chelator to acquire zinc without the need of transporters. TPEN treatment also caused a dramatic increase in intracellular manganese by an unknown mechanism. TPEN likely has biological effects independent of zinc chelation, a limitation that has recently called into question its use as an inducer of zinc deficiency.<sup>71,72</sup> Consistent with this, RNA-seq identified 1341 *P. denitrificans* genes differentially expressed in zinc-chelated versus zinc-replete conditions compared to only 147 in zinc-limited conditions.<sup>38</sup> Thus, TPEN induces large scale transcriptional alterations that may not be related solely to zinc deficiency.

In summary, *P. denitrificans* encodes two zinc ABC transporter systems, either of which is sufficient and required for growth in zinc-limited media. We have also demonstrated that the zinc metallochaperone AztD is capable of sequestering zinc under conditions of zinc limitation, likely in the periplasm. ZnuA may also function in this capacity via binding of multiple zinc ions to its long, flexible loop with a high affinity. Although it appears that AztABCD and ZnuABC have redundant roles in

acquiring zinc from limited media, it remains to be seen whether these proteins serve distinct functions in acquiring zinc from different environments.

## ■ ASSOCIATED CONTENT

### 📄 Supporting Information

The Supporting Information is available free of charge on the ACS Publications website at DOI: 10.1021/acs.biochem.8b00854.

Operon map of *aztABCD* and *znuABC*, multiple sequence alignment of cluster A-I solute binding proteins, and RT-PCR for *aztD* expression in WT and mutant strains (PDF)

## ■ AUTHOR INFORMATION

### Corresponding Author

\*E-mail: [etyukl@nmsu.edu](mailto:etyukl@nmsu.edu). Tel: 575-646-3176.

### ORCID

Erik T. Yukl: 0000-0001-6519-6938

### Author Contributions

D.P.N. acquired, analyzed, and interpreted data. D.P.N. and S.K. generated knockout strains. E.T.Y. conceived and designed the study. Both D.P.N. and E.T.Y. wrote the manuscript.

### Funding

Research reported in this publication was supported by the National Institute of General Medical Science of the National Institutes of Health (1SC2GM111170-01).

### Notes

The authors declare no competing financial interest.

## ■ ACKNOWLEDGMENTS

We acknowledge Dr. Stephen Spiro at the University of Texas at Dallas for supplying bacterial strains, plasmids, and training for the generation of *Paracoccus denitrificans* knockout strains. We are also grateful to Dr. Pradip Saud in the Department of Animal Extension Sciences and Natural Resources at New Mexico State University for statistical assistance.

## ■ REFERENCES

- (1) Coleman, J. E. (1992) Zinc proteins: enzymes, storage proteins, transcription factors, and replication proteins. *Annu. Rev. Biochem.* 61, 897–946.
- (2) Vallee, B. L., and Falchuk, K. H. (1993) The biochemical basis of zinc physiology. *Physiol. Rev.* 73, 79–118.
- (3) Capdevila, D. A., Wang, J., and Giedroc, D. P. (2016) Bacterial Strategies to Maintain Zinc Metallostasis at the Host-Pathogen Interface. *J. Biol. Chem.* 291, 20858–20868.
- (4) Kehl-Fie, T. E., and Skaar, E. P. (2010) Nutritional immunity beyond iron: a role for manganese and zinc. *Curr. Opin. Chem. Biol.* 14, 218–224.
- (5) Bobrov, A. G., Kirillina, O., Fetherston, J. D., Miller, M. C., Burlison, J. A., and Perry, R. D. (2014) The *Yersinia pestis* siderophore, yersiniabactin, and the ZnuABC system both contribute to zinc acquisition and the development of lethal septicemic plague in mice. *Mol. Microbiol.* 93, 759–775.
- (6) Grim, K. P., San Francisco, B., Radin, J. N., Brazel, E. B., Kelliher, J. L., Parraga Solorzano, P. K., Kim, P. C., McDevitt, C. A., and Kehl-Fie, T. E. (2017) The Metallophore Staphylopin Enables *Staphylococcus aureus* To Compete with the Host for Zinc and Overcome Nutritional Immunity. *mBio* 8, 01281.
- (7) Mastropasqua, M. C., D’Orazio, M., Cerasi, M., Pacello, F., Gismondi, A., Canini, A., Canuti, L., Consalvo, A., Ciavardelli, D.,

Chirullo, B., Pasquali, P., and Battistoni, A. (2017) Growth of *Pseudomonas aeruginosa* in zinc poor environments is promoted by a nicotianamine-related metallophore. *Mol. Microbiol.* 106, 543–561.

(8) Gaither, L. A., and Eide, D. J. (2001) Eukaryotic zinc transporters and their regulation. *BioMetals* 14, 251–270.

(9) Cerasi, M., Liu, J. Z., Ammendola, S., Poe, A. J., Petrarca, P., Pesciaroli, M., Pasquali, P., Raffatelli, M., and Battistoni, A. (2014) The ZupT transporter plays an important role in zinc homeostasis and contributes to *Salmonella enterica* virulence. *Metallomics* 6, 845–853.

(10) Sabri, M., Houle, S., and Dozois, C. M. (2009) Roles of the extraintestinal pathogenic *Escherichia coli* ZnuACB and ZupT zinc transporters during urinary tract infection. *Infect. Immun.* 77, 1155–1164.

(11) Lewinson, O., Lee, A. T., and Rees, D. C. (2009) A P-type ATPase importer that discriminates between essential and toxic transition metals. *Proc. Natl. Acad. Sci. U. S. A.* 106, 4677–4682.

(12) Rosadini, C. V., Gawronski, J. D., Raimunda, D., Arguello, J. M., and Akerley, B. J. (2011) A novel zinc binding system, ZevAB, is critical for survival of nontypeable *Haemophilus influenzae* in a murine lung infection model. *Infect. Immun.* 79, 3366–3376.

(13) Klein, J. S., and Lewinson, O. (2011) Bacterial ATP-driven transporters of transition metals: physiological roles, mechanisms of action, and roles in bacterial virulence. *Metallomics* 3, 1098–1108.

(14) Biemans-Oldehinkel, E., Doeven, M. K., and Poolman, B. (2006) ABC transporter architecture and regulatory roles of accessory domains. *FEBS Lett.* 580, 1023–1035.

(15) Higgins, C. F. (1992) ABC transporters: from microorganisms to man. *Annu. Rev. Cell Biol.* 8, 67–113.

(16) van der Heide, T., and Poolman, B. (2002) ABC transporters: one, two or four extracytoplasmic substrate-binding sites? *EMBO Rep.* 3, 938–943.

(17) Khare, D., Oldham, M. L., Orelle, C., Davidson, A. L., and Chen, J. (2009) Alternating access in maltose transporter mediated by rigid-body rotations. *Mol. Cell* 33, 528–536.

(18) Berntsson, R. P., Smits, S. H., Schmitt, L., Slotboom, D. J., and Poolman, B. (2010) A structural classification of substrate-binding proteins. *FEBS Lett.* 584, 2606–2617.

(19) Lu, D., Boyd, B., and Lingwood, C. A. (1997) Identification of the key protein for zinc uptake in *Haemophilus influenzae*. *J. Biol. Chem.* 272, 29033–29038.

(20) Campoy, S., Jara, M., Busquets, N., Perez De Rozas, A. M., Badiola, I., and Barbe, J. (2002) Role of the high-affinity zinc uptake znuABC system in *Salmonella enterica* serovar typhimurium virulence. *Infect. Immun.* 70, 4721–4725.

(21) Garrido, M. E., Bosch, M., Medina, R., Llagostera, M., Perez de Rozas, A. M., Badiola, I., and Barbe, J. (2003) The high-affinity zinc-uptake system znuACB is under control of the iron-uptake regulator (*fur*) gene in the animal pathogen *Pasteurella multocida*. *FEMS Microbiol. Lett.* 221, 31–37.

(22) Kim, S., Watanabe, K., Shirahata, T., and Watarai, M. (2004) Zinc uptake system (*znuA* locus) of *Brucella abortus* is essential for intracellular survival and virulence in mice. *J. Vet. Med. Sci.* 66, 1059–1063.

(23) Ammendola, S., Pasquali, P., Pistoia, C., Petrucci, P., Petrarca, P., Rotilio, G., and Battistoni, A. (2007) High-affinity Zn<sup>2+</sup> uptake system ZnuABC is required for bacterial zinc homeostasis in intracellular environments and contributes to the virulence of *Salmonella enterica*. *Infect. Immun.* 75, 5867–5876.

(24) Corbett, D., Wang, J., Schuler, S., Lopez-Castejon, G., Glenn, S., Brough, D., Andrew, P. W., Cavet, J. S., and Roberts, I. S. (2012) Two zinc uptake systems contribute to the full virulence of *Listeria monocytogenes* during growth in vitro and in vivo. *Infect. Immun.* 80, 14–21.

(25) Sheng, Y., Fan, F., Jensen, O., Zhong, Z., Kan, B., Wang, H., and Zhu, J. (2015) Dual Zinc Transporter Systems in *Vibrio cholerae* Promote Competitive Advantages over Gut Microbiome. *Infect. Immun.* 83, 3902–3908.

- (26) Dintilhac, A., Alloing, G., Granadel, C., and Claverys, J. P. (1997) Competence and virulence of *Streptococcus pneumoniae*: Adc and PsaA mutants exhibit a requirement for Zn and Mn resulting from inactivation of putative ABC metal permeases. *Mol. Microbiol.* 25, 727–739.
- (27) Plumptre, C. D., Eijkelkamp, B. A., Morey, J. R., Behr, F., Counago, R. M., Ogunniyi, A. D., Kobe, B., O'Mara, M. L., Paton, J. C., and McDevitt, C. A. (2014) AdcA and AdcAII employ distinct zinc acquisition mechanisms and contribute additively to zinc homeostasis in *Streptococcus pneumoniae*. *Mol. Microbiol.* 91, 834–851.
- (28) Tedde, V., Rosini, R., and Galeotti, C. L. (2016) Zn<sup>2+</sup> Uptake in *Streptococcus pyogenes*: Characterization of adcA and lmb Null Mutants. *PLoS One* 11, e0152835.
- (29) Bersch, B., Bougault, C., Roux, L., Favier, A., Vernet, T., and Durmort, C. (2013) New insights into histidine triad proteins: solution structure of a *Streptococcus pneumoniae* PhtD domain and zinc transfer to AdcAII. *PLoS One* 8, e81168.
- (30) Eijkelkamp, B. A., Pederick, V. G., Plumptre, C. D., Harvey, R. M., Hughes, C. E., Paton, J. C., and McDevitt, C. A. (2016) The First Histidine Triad Motif of PhtD Is Critical for Zinc Homeostasis in *Streptococcus pneumoniae*. *Infect. Immun.* 84, 407–415.
- (31) Ogunniyi, A. D., Grabowicz, M., Mahdi, L. K., Cook, J., Gordon, D. L., Sadlon, T. A., and Paton, J. C. (2009) Pneumococcal histidine triad proteins are regulated by the Zn<sup>2+</sup>-dependent repressor AdcR and inhibit complement deposition through the recruitment of complement factor H. *FASEB J.* 23, 731–738.
- (32) Ilari, A., Alaleona, F., Tria, G., Petrarca, P., Battistoni, A., Zamparelli, C., Verzili, D., Falconi, M., and Chiancone, E. (2014) The *Salmonella enterica* ZinT structure, zinc affinity and interaction with the high-affinity uptake protein ZnuA provide insight into the management of periplasmic zinc. *Biochim. Biophys. Acta, Gen. Subj.* 1840, 535–544.
- (33) Petrarca, P., Ammendola, S., Pasquali, P., and Battistoni, A. (2010) The Zur-regulated ZinT protein is an auxiliary component of the high-affinity ZnuABC zinc transporter that facilitates metal recruitment during severe zinc shortage. *J. Bacteriol.* 192, 1553–1564.
- (34) Gabbianelli, R., Scotti, R., Ammendola, S., Petrarca, P., Nicolini, L., and Battistoni, A. (2011) Role of ZnuABC and ZinT in *Escherichia coli* O157:H7 zinc acquisition and interaction with epithelial cells. *BMC Microbiol.* 11, 36.
- (35) Graham, A. I., Hunt, S., Stokes, S. L., Bramall, N., Bunch, J., Cox, A. G., McLeod, C. W., and Poole, R. K. (2009) Severe zinc depletion of *Escherichia coli*: roles for high affinity zinc binding by ZinT, zinc transport and zinc-independent proteins. *J. Biol. Chem.* 284, 18377–18389.
- (36) Panina, E. M., Mironov, A. A., and Gelfand, M. S. (2003) Comparative genomics of bacterial zinc regulons: enhanced ion transport, pathogenesis, and rearrangement of ribosomal proteins. *Proc. Natl. Acad. Sci. U. S. A.* 100, 9912–9917.
- (37) Cao, K., Li, N., Wang, H., Cao, X., He, J., Zhang, B., He, Q. Y., Zhang, G., and Sun, X. (2018) Two zinc-binding domains in the transporter AdcA from *J. Biol. Chem.* 293, 6075–6089.
- (38) Neupane, D. P., Jacquez, B., Sundararajan, A., Ramaraj, T., Schilkey, F. D., and Yukl, E. T. (2017) Zinc-Dependent Transcriptional Regulation in *Paracoccus denitrificans*. *Front. Microbiol.* 8, 569.
- (39) Claverys, J. P. (2001) A new family of high-affinity ABC manganese and zinc permeases. *Res. Microbiol.* 152, 231–243.
- (40) Loisel, E., Jacquamet, L., Serre, L., Bauvois, C., Ferrer, J. L., Vernet, T., Di Guilmi, A. M., and Durmort, C. (2008) AdcAII, a new pneumococcal Zn-binding protein homologous with ABC transporters: biochemical and structural analysis. *J. Mol. Biol.* 381, 594–606.
- (41) Banerjee, S., Wei, B., Bhattacharyya-Pakrasi, M., Pakrasi, H. B., and Smith, T. J. (2003) Structural determinants of metal specificity in the zinc transport protein ZnuA from *synechocystis* 6803. *J. Mol. Biol.* 333, 1061–1069.
- (42) Wei, B., Randich, A. M., Bhattacharyya-Pakrasi, M., Pakrasi, H. B., and Smith, T. J. (2007) Possible regulatory role for the histidine-rich loop in the zinc transport protein, ZnuA. *Biochemistry* 46, 8734–8743.
- (43) Yatsunyk, L. A., Easton, J. A., Kim, L. R., Sugarbaker, S. A., Bennett, B., Breece, R. M., Vorontsov, I. I., Tierney, D. L., Crowder, M. W., and Rosenzweig, A. C. (2008) Structure and metal binding properties of ZnuA, a periplasmic zinc transporter from *Escherichia coli*. *JBIC, J. Biol. Inorg. Chem.* 13, 271–288.
- (44) Handali, M., Roychowdhury, H., Neupane, D. P., and Yukl, E. T. (2015) AztD, a Periplasmic Zinc Metallochaperone to an ATP-binding Cassette (ABC) Transporter System in *Paracoccus denitrificans*. *J. Biol. Chem.* 290, 29984–29992.
- (45) Neupane, D. P., Avalos, D., Fullam, S., Roychowdhury, H., and Yukl, E. T. (2017) Mechanisms of zinc binding to the solute-binding protein AztC and transfer from the metallochaperone AztD. *J. Biol. Chem.* 292, 17496–17505.
- (46) Handali, M., Neupane, D. P., Roychowdhury, H., and Yukl, E. T. (2015) Transcriptional Regulation, Metal Binding Properties and Structure of Pden1597, an Unusual Zinc Transport Protein from *Paracoccus denitrificans*. *J. Biol. Chem.* 290, 11878–11889.
- (47) Wang, Y., Graichen, M. E., Liu, A., Pearson, A. R., Wilmot, C. M., and Davidson, V. L. (2003) MauG, a novel diheme protein required for tryptophan tryptophylquinone biogenesis. *Biochemistry* 42, 7318–7325.
- (48) Edelhoch, H. (1967) Spectroscopic determination of tryptophan and tyrosine in proteins. *Biochemistry* 6, 1948–1954.
- (49) Golynskiy, M. V., Gunderson, W. A., Hendrich, M. P., and Cohen, S. M. (2006) Metal binding studies and EPR spectroscopy of the manganese transport regulator MntR. *Biochemistry* 45, 15359–15372.
- (50) Kuzmic, P. (1996) Program DYNAFIT for the analysis of enzyme kinetic data: application to HIV proteinase. *Anal. Biochem.* 237, 260–273.
- (51) Kuzmic, P. (2009) DynaFit—a software package for enzymology. *Methods Enzymol.* 467, 247–280.
- (52) Schafer, A., Tauch, A., Jager, W., Kalinowski, J., Thierbach, G., and Puhler, A. (1994) Small mobilizable multi-purpose cloning vectors derived from the *Escherichia coli* plasmids pK18 and pK19: selection of defined deletions in the chromosome of *Corynebacterium glutamicum*. *Gene* 145, 69–73.
- (53) Sullivan, M. J., Gates, A. J., Appia-Ayme, C., Rowley, G., and Richardson, D. J. (2013) Copper control of bacterial nitrous oxide emission and its impact on vitamin B12-dependent metabolism. *Proc. Natl. Acad. Sci. U. S. A.* 110, 19926–19931.
- (54) Gibson, D. G., Young, L., Chuang, R. Y., Venter, J. C., Hutchison, C. A., 3rd, and Smith, H. O. (2009) Enzymatic assembly of DNA molecules up to several hundred kilobases. *Nat. Methods* 6, 343–345.
- (55) Team, R. C. (2018) *R: A Language and Environment for Statistical Computing*, R Foundation for Statistical Computing, Vienna, Austria.
- (56) Desrosiers, D. C., Sun, Y. C., Zaidi, A. A., Eggers, C. H., Cox, D. L., and Radolf, J. D. (2007) The general transition metal (Tro) and Zn<sup>2+</sup> (Znu) transporters in *Treponema pallidum*: analysis of metal specificities and expression profiles. *Mol. Microbiol.* 65, 137–152.
- (57) Hazlett, K. R., Rusnak, F., Kehres, D. G., Bearden, S. W., La Vake, C. J., La Vake, M. E., Maguire, M. E., Perry, R. D., and Radolf, J. D. (2003) The *Treponema pallidum* tro operon encodes a multiple metal transporter, a zinc-dependent transcriptional repressor, and a semi-autonomously expressed phosphoglycerate mutase. *J. Biol. Chem.* 278, 20687–20694.
- (58) Sharma, N., Selvakumar, P., Saini, G., Warghane, A., Ghosh, D. K., and Sharma, A. K. (2016) Crystal structure analysis in Zn<sup>2+</sup>-bound state and biophysical characterization of CLas-ZnuA2. *Biochim. Biophys. Acta, Proteins Proteomics* 1864, 1649–1657.
- (59) Zheng, B., Zhang, Q., Gao, J., Han, H., Li, M., Zhang, J., Qi, J., Yan, J., and Gao, G. F. (2011) Insight into the interaction of metal ions with TroA from *Streptococcus suis*. *PLoS One* 6, e19510.

- (60) Brautigam, C. A. (2015) Fitting two- and three-site binding models to isothermal titration calorimetric data. *Methods* 76, 124–136.
- (61) Kay, A. R. (2004) Detecting and minimizing zinc contamination in physiological solutions. *BMC Physiol.* 4, 4.
- (62) Yatsunyk, L. A., Easton, J. A., Kim, L. R., Sugarbaker, S. A., Bennett, B., Breece, R. M., Vorontsov, I., Tierney, D. L., Crowder, M. W., and Rosenzweig, A. C. (2008) Structure and metal binding properties of ZnuA, a periplasmic zinc transporter from *Escherichia coli*. *JBIC, J. Biol. Inorg. Chem.* 13, 271–288.
- (63) Pederick, V. G., Eijkelkamp, B. A., Begg, S. L., Ween, M. P., McAllister, L. J., Paton, J. C., and McDevitt, C. A. (2015) ZnuA and zinc homeostasis in *Pseudomonas aeruginosa*. *Sci. Rep.* 5, 13139.
- (64) Yükl, E. T. (2017) The Cluster A-I Solute-Binding Proteins. *Encyclopedia of Inorganic and Bioinorganic Chemistry*, 1.
- (65) Auld, D. S. (2001) Zinc coordination sphere in biochemical zinc sites. *BioMetals* 14, 271–313.
- (66) Outten, C. E., and O'Halloran, T. V. (2001) Femtomolar sensitivity of metalloregulatory proteins controlling zinc homeostasis. *Science* 292, 2488–2492.
- (67) Bayle, L., Chimalapati, S., Schoehn, G., Brown, J., Vernet, T., and Durmort, C. (2011) Zinc uptake by *Streptococcus pneumoniae* depends on both AdcA and AdcAII and is essential for normal bacterial morphology and virulence. *Mol. Microbiol.* 82, 904–916.
- (68) Nokhal, T.-H., and Schlegel, H. G. (1983) Taxonomic Study of *Paracoccus denitrificans*. *Int. J. Syst. Bacteriol.* 33, 26–37.
- (69) Noulas, C., Tziouvalekas, M., and Karyotis, T. (2018) Zinc in soils, water and food crops. *J. Trace Elem. Med. Biol.* 49, 252–260.
- (70) Luxton, T., Miller, B., and Scheckel, K. (2013) *Zinc Speciation Studies in Soil, Sediment and Environmental Samples*, 443.
- (71) Richardson, C. E. R., Cunden, L. S., Butty, V. L., Nolan, E. M., Lippard, S. J., and Shoulders, M. D. (2018) A Method for Selective Depletion of Zn(II) Ions from Complex Biological Media and Evaluation of Cellular Consequences of Zn(II) Deficiency. *J. Am. Chem. Soc.* 140, 2413–2416.
- (72) Bozym, R. A., Thompson, R. B., Stoddard, A. K., and Fierke, C. A. (2006) Measuring picomolar intracellular exchangeable zinc in PC-12 cells using a ratiometric fluorescence biosensor. *ACS Chem. Biol.* 1, 103–111.